Ballistic transport and electrical spin signal enhancement in a nanoscale three-terminal spintronic device

Lei Zhu and Edward T. Yu[a)]
Department of Electrical and Computer Engineering Microelectronics Research Center, The University of Texas at Austin, Austin, Texas 78758, USA

(Received 6 August 2010; accepted 26 February 2011; published online 7 April 2011)

Ballistic electron transport at nanoscale dimensions is investigated and exploited in a nanoscale three-terminal, all-electrical spintronic semiconductor device. Charge current cancellation under appropriate device biasing yields a large, spin-dependent current signal even with modest spin injection efficiency into the semiconductor, while reliance on ballistic, rather than diffusive, carrier transport is expected to enable robust scalability to smaller dimensions. Magnetocurrent in excess of 200% is measured with spin injection efficiency of 5%, and a spin-dependent ballistic carrier transport model is shown to yield accurate, quantitative predictions of current-voltage behavior. © *2011 American Institute of Physics*. [doi:10.1063/1.3567922]

Information processing based on transport and manipulation of electron spin, rather than charge, in semiconductors offers the promise of dramatic advances in speed, power consumption, and functionality of solid-state electronic devices.[1] However, challenges abound in the attainment of highly efficient electrical injection of spin-polarized electrons into a semiconductor, robust manipulation and detection of electron spin, and realization of electrical device concepts readily scalable to nanoscale dimensions.[2,3] Numerous ferromagnet/semiconductor hybrid electrical devices have been designed and experimentally demonstrated[4–6] but frequently with performance limitations imposed by the low efficiency of spin injection and extraction, and demanding requirements for retention of spin polarization within the semiconductor. Multiterminal electrical device structures have also been proposed,[7–10] and investigated experimentally,[11–13] based on operation in the diffusive regime of electron transport within the semiconductor. However, the dependence on diffusive transport complicates scalability to dimensions at which transport may occur in the ballistic, rather than the diffusive, regime.

In this letter, we report demonstration and analysis of a three-terminal, all-electrical spintronic switching device in which ballistic electron transport at nanoscale dimensions combined with charge current cancellation by appropriate device biasing yields a robust, electrically enhanced spin-dependent current signal despite modest efficiency in electrical injection of spin-polarized electrons. The basic device structure employed is shown in Fig. 1. Three ferromagnetic contacts are fabricated on a p-type InAs semiconductor surface, enabling electrical injection of a partially spin-polarized electron current into the two-dimensional electron inversion layer formed at the InAs surface.[14] The physical dimensions of the device are such that electron transport between adjacent contacts is ballistic rather than diffusive, leading to fundamental differences in device behavior, an increase in spin dependence of current flow, and improved scalability to smaller dimensions. Compared, for example, with the dual-drain nonlocal lateral spin device of Ref. 13, which has a nominally similar geometry, the device described here employs a very different mechanism of operation and functions in the ballistic, rather than diffusive, carrier transport regime.

Our devices were fabricated on p-type InAs (100) wafers with the surface passivated in a sulfur saturated ammonium sulfide solution for 15 min at room temperature.[15] A layer of Al_2O_3 ~3 nm in thickness was then deposited by rf sputter-

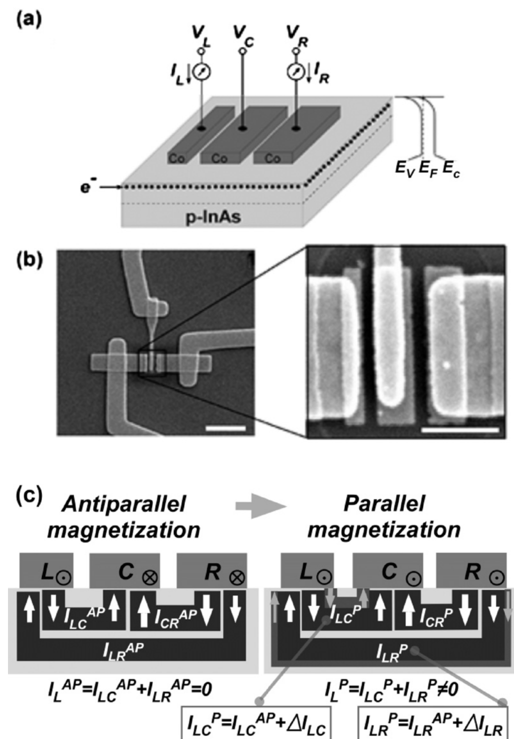

FIG. 1. (a) Schematic diagram of three-terminal device geometry and measurement configuration. (b) Scanning electron microscope image of device with Co contacts and Au leads on p-InAs; magnified view shows geometry and dimensions of the three Co contacts. Scale bars are 2 μm (left) and 500 nm (right). (c) Current distributions in the three-terminal device. Current flow paths are indicated schematically by the dark shaded regions, with their widths indicating the current magnitude, and the arrows indicating the direction of electrical current flow. As shown, current flow at the left terminal increases from zero for antiparallel magnetization ($I_L^{AP}=0$) to nonzero for parallel magnetization ($I_L^{P}\neq 0$).

a)Author to whom correspondence should be addressed: Electronic mail: ety@ece.utexas.edu.

 © 2011 American Institute of Physics

Author complimentary copy. Redistribution subject to AIP license or copyright, see http://apl.aip.org/apl/copyright.jsp

ing 30 nm Co ferromagnetic contacts were fabricated by electron-beam lithography and a standard metal deposition/liftoff process. The basic operational concept for the device is as follows. Bias voltages V_L, V_C, and V_R are applied to the left, center, and right contact terminals, respectively, as shown in Fig. 1. In the ballistic transport regime, the total charge current at one terminal includes contributions from electron transport between that terminal and the two other terminals, and in both spin up and spin down electron channels. Thus, the current at the left terminal, I_L, is given by

$$I_L = I_{LC} + I_{LR} = \sum_{\alpha,\beta} (I_{LC}^{\alpha\beta} + I_{LR}^{\alpha\beta}), \quad (1)$$

where I_{LC} and I_{LR} represent the charge current flowing from the left terminal to the center terminal and the right terminal, respectively, and $I_{LC}^{\alpha\beta}$ and $I_{LR}^{\alpha\beta}$ represent the current from spin channel α at the left terminal to spin channel β at the center terminal and at the right terminal, respectively. Similarly, $I_C = \Sigma_{\alpha,\beta}(I_{CR}^{\alpha\beta} - I_{LC}^{\alpha\beta})$ and $I_R = \Sigma_{\alpha,\beta}(-I_{CR}^{\alpha\beta} - I_{LR}^{\alpha\beta})$. Because $I_{LC}^{\alpha\beta}$, $I_{LR}^{\alpha\beta}$, and $I_{CR}^{\alpha\beta}$ are dependent on the relative magnetization directions of each pair of terminals, I_L, I_C, and I_R can be modulated via the magnetizations of the three contacts as well as by the voltages V_L, V_C, and V_R.

Shape anisotropy associated with the different aspect ratio of the left contact compared to the center and right contacts, as shown in Fig. 1, leads to a higher coercive field for that contact. Thus, the magnetization in the left contact can be made either parallel or antiparallel to those of the center and right contacts by application of an appropriate external magnetic field. We, therefore, choose to monitor the current at the left terminal, I_L, to demonstrate magnetocurrent response, with I_L being used to represent the on/off states of the three-terminal device,[16,17] and define the magnetocurrent of the three-terminal device as $MC = (I_L^P - I_L^{AP}) / I_L^{AP}$ with $I_L^P \equiv I_L^{\downarrow\downarrow\downarrow}$, $I_L^{AP} \equiv I_L^{\downarrow\uparrow\uparrow}$, and the arrow superscripts for I_L indicating the magnetization state of the three contacts (left, center, and right).

For a particular contact magnetization state, e.g., the left contact magnetization antiparallel to those of the center and right contacts, the three-terminal device is set to the "off" state with the charge current I_L vanishing under application of appropriate bias voltages. In this situation, the currents I_{LR} and I_{LC} are each nonzero but compensate each other to yield $I_L^{AP} = 0$. If the magnetization of the left contact is then reversed, yielding a configuration for the device "on" state in which all contacts have parallel magnetization, I_{LR} and I_{LC} individually will each change by only a small percentage. However, ΔI_{LC} and ΔI_{LR} are opposite in direction and, more importantly, differ in magnitude, as shown in Fig. 1(c). Therefore, in the device on state, the current at the left terminal, $I_L^P = \Delta I_L = \Delta I_{LC} + \Delta I_{LR}$, becomes nonzero. Although comparable values of ΔI_L can also be attained in a conventional two-terminal spin valve geometry, e.g., with only the left and center terminals involved, the large on/off current switching ratio, defined as the magnetocurrent at the left terminal, can only be achieved in the three-terminal device, due to the finite ΔI_L and the near-zero I_L^{AP} in the three-terminal case. In other words, the enhanced magnetocurrent originates from the coexistence of all three terminals, in which, for the off state, the current flowing from the right terminal to the left terminal cancels out the current flowing from the left terminal to the center terminal, resulting in near-zero total current flow at the left terminal.

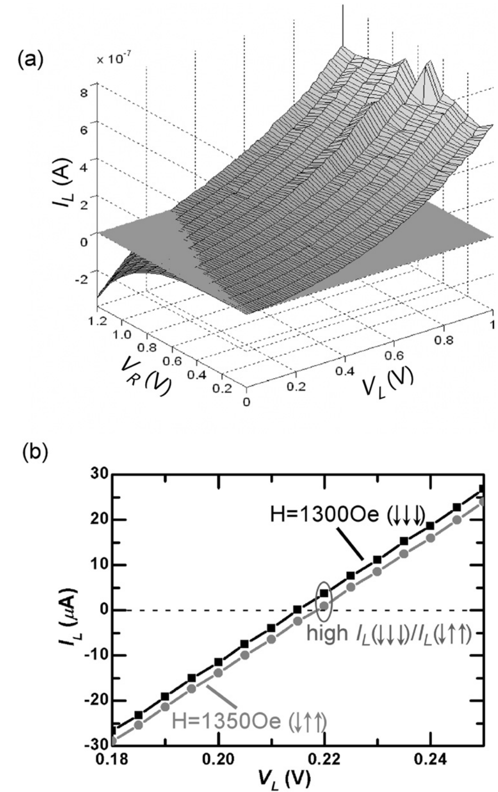

FIG. 2. (a) Contour plot of electrical charge current I_L measured at 4.2 K as a function of voltages V_R and V_L, with $V_C=0$ and zero external magnetic field applied. A locus of points in the (V_R, V_L)-plane corresponding to $I_L=0$ is clearly evident. (b) Shift in I_L due to alterations in spin injection and transport upon application of an external magnetic field that changes the magnetization configuration of the Co contacts. For operation near a point at which $I_L(\downarrow\uparrow\uparrow)=0$, a large on/off current switching ratio can be attained. Data shown were obtained for $V_R=1.00$ V.

Key to efficient operation of this device is scaling of the device to dimensions at which electron transport between adjacent contacts is largely ballistic, rather than diffusive. Results of weak localization/antilocalization measurements at 4.2 K have yielded an elastic scattering length of ~60–90 nm,[18] comparable to the separation between the adjacent contacts, and therefore enabling ballistic electron transport between them. To confirm that the coercive fields for magnetization reversal are different for contacts of different widths, due to shape anisotropy effects, we have used magnetic force microscopy (MFM) to measure the magnetization as a function of external applied magnetic field.[19]

The current I_L, measured as a function of bias voltages V_L and V_R, with $V_C=0$, for a representative three-terminal device with parallel magnetization for all three Co contacts is shown in Fig. 2(a). As expected from the device geometry, there exists a locus of points (V_L, V_R) for which $I_L=0$. When an external magnetic field is applied to reverse the magnetization of the two larger contacts, the curve $I_L(V_L, V_R)$ and, consequently, the locus of points for which $I_L=0$, shifts, as shown in Fig. 2(b), allowing a large magnetocurrent to be realized.

Figure 3 demonstrates this concept. I_L is shown for $V_L=0.220$ V, $V_C=0$, and $V_R=1.000$ V as a function of externally applied magnetic field, for external fields swept from -3000 to $+3000$ Oe (gray diamonds) and $+3000$ to -3000

Author complimentary copy. Redistribution subject to AIP license or copyright, see http://apl.aip.org/apl/copyright.jsp

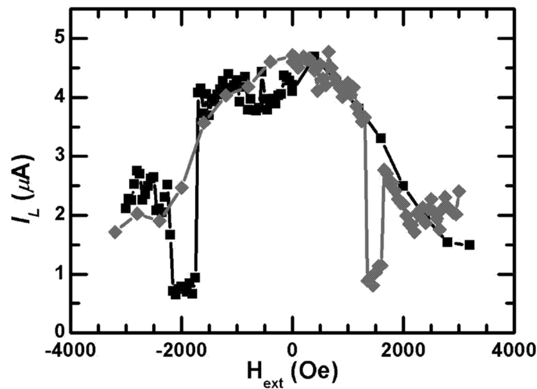

FIG. 3. Electrical charge current flow I_L as a function of external applied magnetic field, for field sweep directions − to + (gray diamonds) and + to − (black squares). A clear shift in current for antiparallel magnetization configurations (↓↑↑ at ~+1500 Oe and ↑↓↓ at ~−2000 Oe) is evident. Adjustment of voltages V_L and V_R allows the current in the antiparallel configuration to approach zero (to within the noise floor of the device), leading to a large on/off current switching ratio.

Oe (black squares). At fields in the vicinity of +1500 Oe (− to +sweep) or −2000 Oe (+ to − sweep) the magnetizations of the two larger contacts are reversed, and the current I_L drops substantially. The measured magnetocurrent MC under this circumstance is 212% for the − to +sweep and 328% for the + to − sweep.

The observed electrical characteristics can be understood quantitatively on the basis of a ballistic electron transport analysis. We apply the standard Landauer–Buttiker formula[20,21] for ballistic transport, modified to accommodate separate spin transport channels and reservoirs.[19,22] The change in I_L that occurs upon changing the magnetization of the left contact relative to that of the center and right contacts is given by

$$\Delta I_L \equiv I_L^P - I_L^{AP} \approx \left(\frac{\gamma^2}{1-\gamma^2}\right)\left(\frac{G_{LC}^P + G_{LC}^{AP}}{2}\right)(V_L - V_C) \times \left[1 - \exp\left(\frac{-L_{LR}}{L_{sf}}\right)\right], \quad (2)$$

where γ is the interface spin-asymmetry coefficient,[23] $I_L^{P(AP)}$ and $G_{LC}^{P(AP)}$ are, respectively, I_L and the left-to-center contact conductance for the left contact magnetization parallel (antiparallel) to the magnetization of the other two contacts, L_{LR} is the left-to-right contact spacing, and L_{sf} is the spin diffusion length in the InAs surface electron layer.

Measurements we performed previously on p-type InAs have yielded $L_{sf}=310\pm130$ nm and $\gamma=5\pm2\%$.[18] Substituting $L_{sf}=310$ nm and $\gamma=5\%$ in Eq. (2) to estimate ΔI_L, we obtain $\Delta I_L\approx2$ μA, in excellent agreement with the observed value of 2–3 μA.

We also model the electrical behavior of this device assuming diffusive carrier motion. Following an analytical model similar to that typically employed for spin valve devices,[19,24] we find that the current change ΔI_L is ~0.1 μA, an order of magnitude smaller than observed in our measurements. The contrast in level of quantitative agreement between our experimental results and analyses based on ballistic and diffusive transport is strong evidence that electron transport in our devices occurs in the ballistic regime. Further analysis and additional evidence confirming the ballistic nature of spin transport are discussed in the supplemental material.[19]

In summary, we have conceived, experimentally demonstrated, and analyzed the behavior of a all-electrical three-terminal spintronic device that provides a large spin-dependent switching signal via ballistic transport at nanoscale dimensions combined with cancellation of charge current under appropriate device biasing. Ballistic electron transport leads to very different spin-dependent current behavior relative to that which would arise from diffusive transport and enables robust scaling to smaller device dimensions. These findings suggest a variety of approaches for the realization of solid-state devices based on electron spin transport and amenable to large-scale integration with conventional semiconductor electronics.

Part of this work was supported by the Office of Naval Research (Grant No. N00014-02-1-1016) and by the University of Texas at Austin.

[1] I. Žutić, J. Fabian, and S. Das Sarma, Rev. Mod. Phys. **76**, 323 (2004).
[2] *Semiconductor Spintronics and Quantum Computation*, Nanoscience and Technology, edited by D. D. Awschalom, D. Loss, and N. Samarth (Springer, Berlin, 2002).
[3] D. D. Awschalom and M. E. Flatte, Nat. Phys. **3**, 153 (2007).
[4] P. R. Hammar, B. R. Bennett, M. J. Yang, and M. Johnson, Phys. Rev. Lett. **83**, 203 (1999).
[5] X. Lou, C. Adelmann, M. Furis, S. A. Crooker, C. J. Palmstrøm, and P. A. Crowell, Phys. Rev. Lett. **96**, 176603 (2006).
[6] C. Ciuti, J. P. McGuire, and L. J. Sham, Phys. Rev. Lett. **89**, 156601 (2002).
[7] J. Fabian and I. Žutić, Phys. Rev. B **69**, 115314 (2004).
[8] H. Dery, Ł. Cywiński, and L. J. Sham, Phys. Rev. B **73**, 161307 (2006).
[9] S.-W. Jung and H.-W. Lee, Phys. Rev. B **73**, 165302 (2006).
[10] H. Dery, P. Dalal, L. Cywinski, and L. J. Sham, Nature (London) **447**, 573 (2007).
[11] G. Meiner, T. Matsuyama, and U. Merkt, Phys. Rev. B **65**, 125327 (2002).
[12] T. Matsuyama, C.-M. Hu, D. Grundler, G. Meier, and U. Merkt, Phys. Rev. B **65**, 155322 (2002).
[13] D. Saha, M. Holub, and P. Bhattacharya, Appl. Phys. Lett. **91**, 072513 (2007).
[14] L. Ö. Olsson, C. B. M. Andersson, M. C. Håkansson, J. Kanski, L. Ilver, and U. O. Karlsson, Phys. Rev. Lett. **76**, 3626 (1996).
[15] D. Y. Petrovykh, M. J. Yang, and L. J. Whitman, Surf. Sci. **523**, 231 (2003).
[16] D. J. Monsma, J. C. Lodder, T. J. A. Popma, and B. Dieny, Phys. Rev. Lett. **74**, 5260 (1995).
[17] R. Jansen, P. S. Anil Kumar, O. M. J. van't Erve, R. Vlutters, P. de Haan, and J. C. Lodder, Phys. Rev. Lett. **85**, 3277 (2000).
[18] L. Zhu and E. T. Yu, J. Vac. Sci. Technol. B **28**, 1164 (2010).
[19] See supplementary material at http://dx.doi.org/10.1063/1.3567922 for magnetic force microscopy measurements on Co terminals, for detailed analytical formulation of spin-dependent transport based on ballistic and drift-diffusion models, and for analysis of potential parasitic effects in a three-terminal spin transistor.
[20] M. Büttiker, Phys. Rev. Lett. **57**, 1761 (1986).
[21] M. Büttiker, IBM J. Res. Dev. **32**, 317 (1988).
[22] H. X. Tang, F. G. Monzon, R. Lifshitz, M. C. Cross, and M. L. Roukes, Phys. Rev. B **61**, 4437 (2000).
[23] A. Fert, J. M. George, H. Jaffrès, and R. Mattana, IEEE Trans. Electron Devices **54**, 921 (2007).
[24] F. J. Jedema, M. S. Nijboer, A. T. Filip, and B. J. van Wees, Phys. Rev. B **67**, 085319 (2003).

Author complimentary copy. Redistribution subject to AIP license or copyright, see http://apl.aip.org/apl/copyright.jsp